Quantum simulation of Abelian models with Rydberg arrays

Yannick Meurice

The University of Iowa
with James Corona, Avi Kaufman, Blake Senseman, Zane Ozzello and M. Asaduzzaman
and collaborators at QuEra, UC Riverside and Chongqing U.
yannick-meurice@uiowa.edu
Supported by the Department of Energy under Award Number DOE DE-SC0019139 and DE-SC0010113

QuantHEP, September 29, 2025

Contents

- The compact Abelian Higgs Model (Scalar QED) and its ladder shaped Rydberg atom simulator (PRD 104, 094513)
- Effective theory for the simulator (PRD 110, 034513 (2024))
- Experimental observation of a “floating" incommensurate phase for the ladder, with QuEra, Nature Communications, 2025 16:712)
- Estimation of entanglement using mutual information of bitstrings from numerical sampling and cloud-based Aquila/Quera operation (arXiv 2404.09935, PRR Letter 7, L022023 (2025))
- Improved entanglement estimators using “filtered" probabilities (arXiv 2411.07092, PRA 112, 032430 (2025))
- Probability distributions of bitstring and dealing with Aquila errors; A. Kaufman et al., arXiv:2507.14128
- Multipartite entanglement estimation (Z. Ozzello et al., arXiv 2507.14422)
- Multiparticle state preparation
- Quantum advantage in 2+1 dimensions using QuEra???

Hybrid hadronization in event generators?

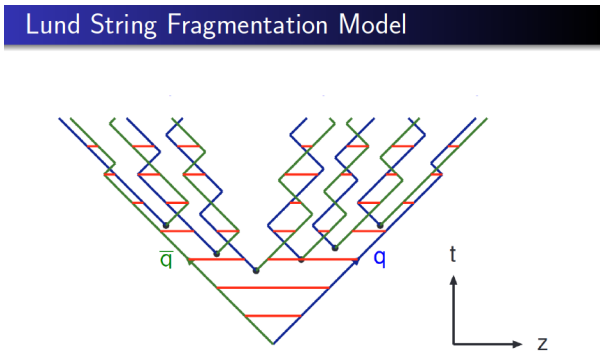

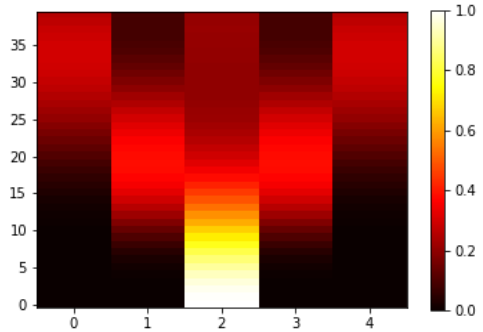

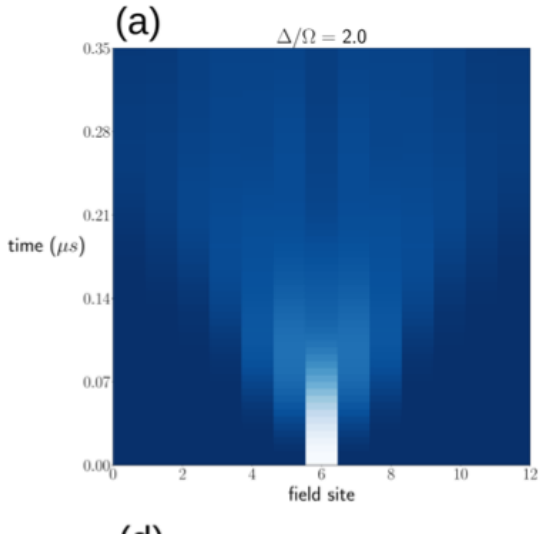

Evolution of a particle-antiparticle pair with the Lund model/Pythia (left), the Abelian Higgs model in 1+1 dimensions (middle), and a Rydberg atom simulator for this model (right). Work in progress towards an hybrid algorithm QuPyth : arXiv:2212.02476 with K. Heitritter (qBraid) and S. Mrenna (Pythia + Fermilab). This model is not intended to be realistic but it is a quantum lattice model (we can compute the entanglement entropy ...)

Climbing the Kogut ladder with TRG and QC

- Real-time scattering for the quantum Ising model with mitigated IBMQ (PRD 99 (2019), Q. Sci.Tech. 6 (2021))
- Phase shifts (PRD 104 (2021), PRD 109 (2024))
- Multiple wave packets (PRD 111 (2025), M. Hite 2505.00476)
- Digitized ϕ^4 (PRD 107 (2023))
- O(2) model with chem. pot. on optical lattices (PRA 90 (2014))
- Abelian Higgs model on optical lattices (PRD 92 (2015))
- Polyakov loop on ladder shaped optical lattices with Rydberg dressing (PRL 121 (2018), PRD 98 (2018))
- Spin-1 Abelian Higgs model with ladder Rydberg arrays and qutrits (PRD 104 (2021) , PRD 110 (2024), Nat. C. 16 (2025))
- Gross-Neveu model with Quantinuum (PRD 106 (2022))
- Quantum Ising model on two-dimensional anti de Sitter space (PRD 109 (2024))

First step: Compact Abelian Higgs Model (CAHM)

$$Z_{CAHM} = \prod_x \int_{-\pi}^{\pi} \frac{d\varphi_x}{2\pi} \prod_{x,\mu} \int_{-\pi}^{\pi} \frac{dA_{x,\mu}}{2\pi} e^{-S_{gauge}-S_{matter}},$$

$$S_{gauge} = \beta_{plaquette} \sum_{x,\mu<\nu} (1 - \cos(A_{x,\mu} + A_{x+\hat{\mu},\nu} - A_{x+\hat{\nu},\mu} - A_{x,\nu})),$$

$$S_{matter} = \beta_{link} \sum_{x,\mu} (1 - \cos(\varphi_{x+\hat{\mu}} - \varphi_x + A_{x,\mu})).$$

- local invariance: $\varphi'_x = \varphi_x + \alpha_x$ and $A'_{x,\mu} = A_{x,\mu} - (\alpha_{x+\hat{\mu}} - \alpha_x)$.
- φ is the Nambu-Goldstone mode of the original model. The Brout-Englert-Higgs mode is decoupled (heavy).
- Discrete Tensor Lattice Field Theory (TLFT) formulation (character expansion, Fourier modes): Gauss's law removes matter quantum numbers (like in the unitary gauge) and truncations do not break symmetries but may affect criticality (see RMP 94, 025005)
- Implementations with cold atoms: see PRD 92, PRL 121, PRD 104

Ab-initio lattice model

Tensor Lattice Field Theory: path integral $\rightarrow$ transfer matrix $\rightarrow$ $\widehat{H}$, see RMP 94

Ab. Higgs: Hamiltonian and Hilbert space in 1+1 dim.

$$H = \frac{U}{2}\sum_{i=1}^{N_s}(L_i^z)^2 + \frac{Y}{2}\sum_i (L_{i+1}^z - L_i^z)^2 - X\sum_{i=1}^{N_s} U_i^x$$

with $U^x \equiv \frac{1}{2}(U^+ + U^-)$ and $L^z|m\rangle = m|m\rangle$ and $U^\pm|m\rangle = |m \pm 1\rangle$.

- m is a discrete electric field quantum number ($-\infty < m < +\infty$)
- In practice, we need to apply truncations: $U^\pm|\pm m_{max}\rangle = 0$
- We focus on the spin-1 truncation ($m = \pm 1, 0$ and $U^x = L^x/\sqrt{2}$).
- Implemented with two blockaded Rydberg atoms (YM PRD 104)
- U-term: electric field energy ($U \to 0$: $O(2)$ in dual form)
- Y-term: matter charges (determined by Gauss's law)
- $Y \to \infty$: pure gauge
- X-term: currents inducing temporal changes in the electric field

Qutrit for scalar QED (UIowa-Rochester-LBNL)

Qutrit: 3 state QPU; L^z: spin-1 rotations

$$\exp(i\gamma L_0^z \otimes L_1^z) = \text{CSUM}^{01} D_1^0 \, \text{CSUM}^{01} D_2^0 \, \text{CSUM}^{01}$$

$$\text{CSUM}^{01} = H^1 \, \text{C}\phi^{01} \, H^1$$

$$D_1^0 = \exp(i\frac{2\gamma}{3} s_z^{01}) \exp(i\frac{\gamma}{3} s_z^{12}), \qquad D_2^0 = \exp(i\frac{\gamma}{3} s_z^{01}) \exp(i\frac{2\gamma}{3} s_z^{12})$$

RC + Purification using globally depolarizing term only

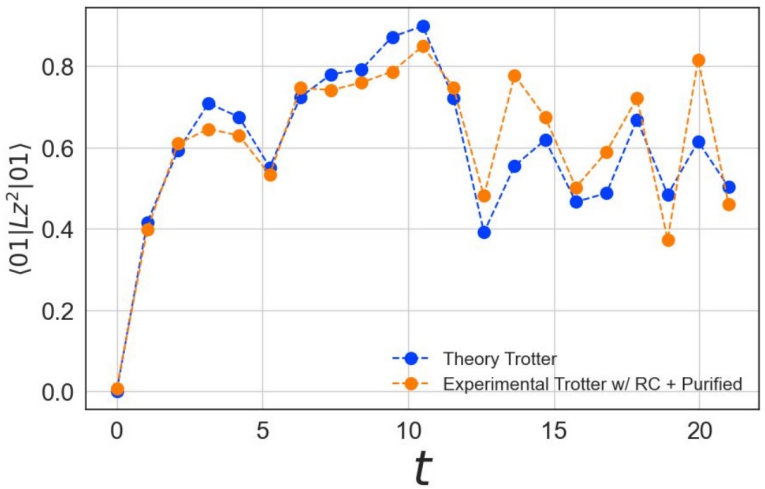

Figure: Preliminary two qutrit evolution using LBNL facilities with various error mitigation methods (Noah Goss).

Ladder of Rydber atoms

One can adapt (Y.M., PRD 104) the optical lattice construction (J. Zhang et al. PRL 121, A. Bazavov et al. PRD 92) using a ladder of ^{87}Rb atoms to simulate the Abelian Higgs model. The Hamiltonian is

$H = \frac{\Omega}{2}\sum_i(|g_i\rangle\langle r_i| + |r_i\rangle\langle g_i|) - \Delta\sum_i n_i + \sum_{i<j} V_{ij} n_i n_j,$
with $|g\rangle$ and $|r\rangle$ the ground and Rydberg states (as qubit), and
Ω: Rabi frequency; Δ: detuning; $V_{ij} = \Omega R_b^6/r_{ij}^6$, the Rydberg potential
When $r = R_b$, the Rydberg radius, $V = \Omega$.
$n|r\rangle = |r\rangle$; $n|g\rangle = 0$.
For rungs small enough, the blockade provides a spin-1:
$|gg\rangle \to |m = 0\rangle$, $|rg\rangle \to |m = 1\rangle$, $|gr\rangle \to |m = -1\rangle$, $|rr\rangle$ decouples

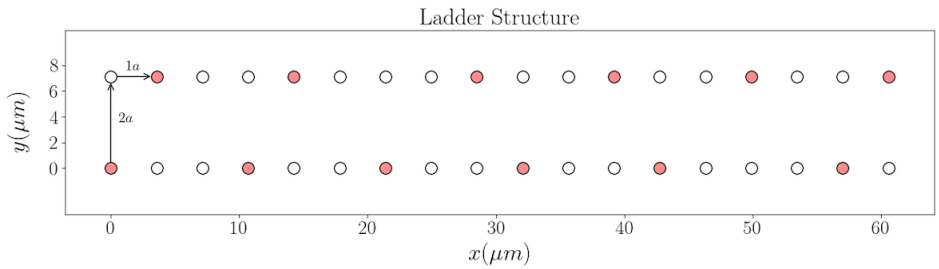

Comparison between ladder $H_{eff.}$ and H_{CAHM} Phys.Rev.D 110 (2024) 3, 034513 arXiv 2312.04436

$$H_{CAHM} = \frac{U}{2}\sum_{i=1}^{N_s}\left(L_i^z\right)^2 - Y\sum_{i=1}^{N_s-1} L_{i+1}^z L_i^z - X\sum_{i=1}^{N_s} U_i^x$$

$$H_{eff.} = -\Delta\sum_{i=1}^{N_s}(L_i^z)^2 + \frac{V_1-V_2}{2}\sum_{i=1}^{N_s-1} L_i^z L_{i+1}^z + \Omega\sum_{i=1}^{N_s} U_i^x + H_{quartic}$$

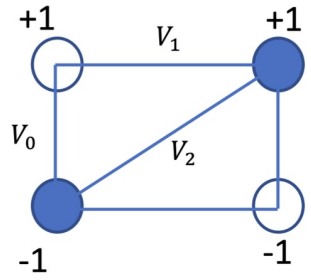

$$H_{quartic} = \frac{V_1+V_2}{2}\sum_{i=1}^{N_s-1}\left(L_i^z\right)^2\left(L_{i+1}^z\right)^2.$$

- $\Delta = -U/2$ (sign matters, penalizes electric flux)
- The coefficient for $L_i^z L_{i+1}^z$ is positive ($V_1 > V_2$) for the simulator (repulsive/antiferromagnetic) but the CAHM has ferromagnetic interactions. This can be remedied by redefining the observable $L_{2i+1}^z \to -L_{2i+1}^z$ (staggered)
- After redefinition $V_1 = -V_2 = Y > 0$ but $V_2 > 0$!
- $\Omega = -X$ (sign does not matter)

Long stories short

- Rich phase diagram at $\Delta > 0$, critical points, continuum limits ...
- $\Delta > 0$ can be used for multiparticle state preparation
- Experimental observation of a “floating" incommensurate phase for the ladder, with QuEra, Nature Communications, 2025 16:712)
- Phase boundaries from bitstring correlations and full quantum wave function are very similar
- Phase diagram: R_b/a versus Δ/Ω

Exp. evidence for a floating phase (J. Zhang, S. Cantu, QuEra, YM, SW. Tsai, Nature Comm. 16:712)

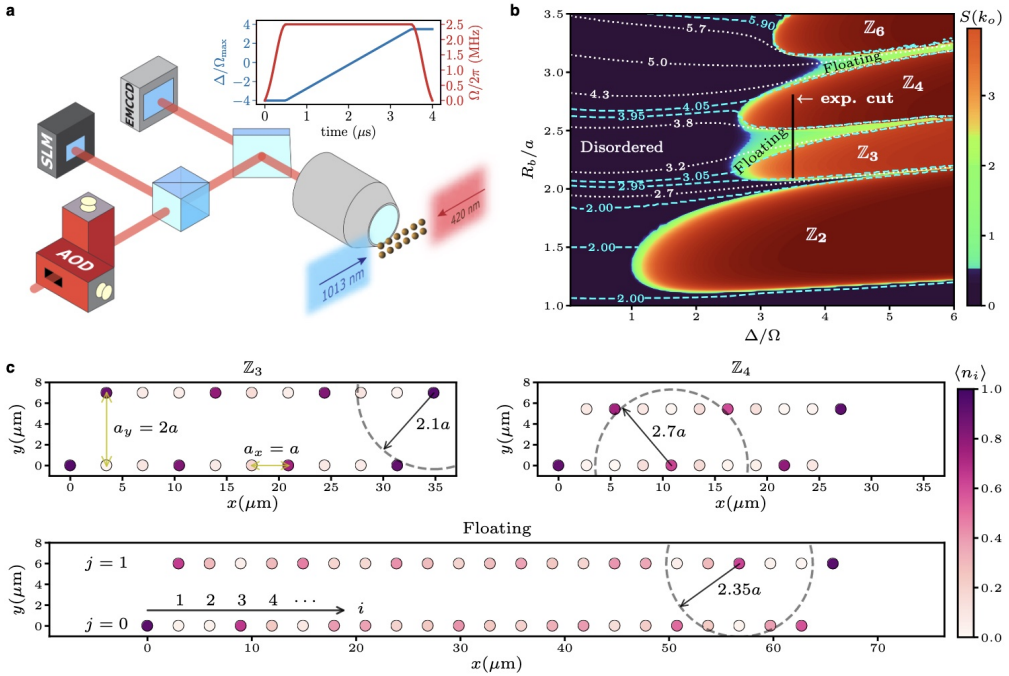

FIG. 1. **Quantum phases of Rydberg atoms arranged in a two-leg ladder. a**, Atoms are loaded into a two-leg ladder of optical tweezer traps generated using a SLM and rearranged into defect-free patterns by a second set of moving tweezers using a pair of crossed AODs. Coherent transitions are driven between the ground state $|g\rangle = |5S_{1/2}\rangle$ and the Rydberg state $|r\rangle = |70S_{1/2}\rangle$ in each atom with a two-photon transition induced by lasers at 420 nm and 1013 nm. The inset shows a linear detuning sweep $\Delta(t)$ at a constant Rabi frequency $\Omega_{\max} = 2\pi \times 2.5\,\mathrm{MHz}$ for preparing the ground states of the phase diagram via adiabatic evolution. Projection of the many-body quantum state into bitstrings of $|g\rangle$ and $|r\rangle$ for each atom can be detected on an EMCCD camera with the Rydberg state $|r\rangle$ detected as loss of atom. **b**, The ground-state phase diagram for the Rydberg Hamiltonian [Eq. (1)] in a two-leg ladder is shown with lattice spacings $a_x = a$ and $a_y = 2a$. Structure factors $S(k)$ are numerically computed for $1 \le R_b/a \le 3.5$ using DMRG (Supplementary Information). The color map depicts the peak height $S(k_o)$ at $k_o = 2\pi/p$ with p being the wavelength in units of the lattice constant a, while contour lines show the constant-p lines. The $\mathbb{Z}_p$ orders have constant values of integer p, while the floating phase exhibits a continuously varying p.

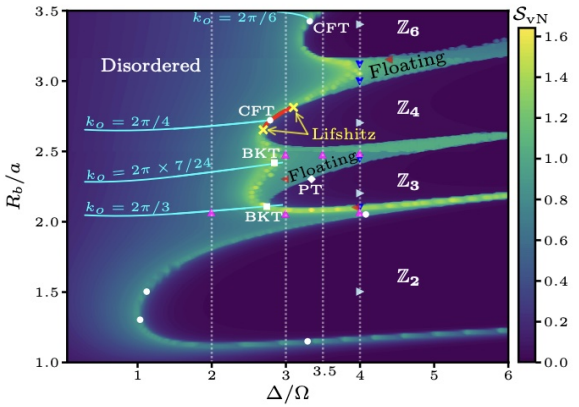

FIG. 7. **Ground-state phase diagram using von Neumann entanglement entropy.** The results for $1 \le R_b/a \le 2.5$, $2.5 < R_b/a \le 3.15$, and $3.15 < R_b/a \le 3.5$ are computed for systems with $L = 288$, 285, and 290, respectively (Fig. 1**b** in the main text also employs this technique). Slight variations in L in different regimes ensure compatibility with the periods of the crystalline orders. The dark lobes represent crystalline orders, and the green areas between crystalline orders, bounded by the bright yellow lines, show the floating phase. The bright yellow lines are BKT transition lines, separating the floating phases and the disordered phase. The boundaries between the floating phases and the crystalline orders are PT transition lines. The red line labels the direct phase transition between the $\mathbb{Z}_4$ order and the disordered phase, which is a chiral transition line with continuously varying critical exponents plus a single CFT point (white circle). The chiral transition line terminates at two Lifshitz points (yellow cross) where the floating phases emerge. There also exist direct phase transitions between the $\mathbb{Z}_6$ order and the disordered phase, which also include a single CFT point. On the equal-k_o lines (cyan lines) in the disordered phase, the peak position of the structure factor $S(k)$ remains constant at k_o. Commensurate lines, where $2\pi/k_o$ is an integer, intersect with the $\mathbb{Z}_{4(6)}$ boundary at the CFT point. The floating phase fully encompasses the $\mathbb{Z}_3$ order, and the $k_o = 2\pi/3$ line goes from the disordered phase into a critical phase and

Entanglement from “experimental" bitstrings?

- Entanglement from a single copy?
- Theorists can run QuEra on the cloud without help
- Is this an “experiment"?
- Output: bitstrings: 00110100010010...(0: ground ; 1: Rydberg)
- Shannon entropy and mutual information for bitsring are “cheap"
- We need to understand and mitigate the errors
- Can we get reliable results with a few thousands shots?

Lattice QCD: reliable results from a few thousands gauge configurations. Can we do the same with quantum simulators? The answer is yes!

PHYSICAL REVIEW D **100,** 034501 (2019)

$B_s \to K\ell\nu$ decay from lattice QCD

A. Bazavov,[1] C. Bernard,[2] C. DeTar,[3] Daping Du,[4] A. X. El-Khadra,[5,6] E. D. Freeland,[7] E. Gámiz,[8] Z. Gelzer,[5] Steven Gottlieb,[9] U. M. Heller,[10] A. S. Kronfeld,[6,11] J. Laiho,[4] Yuzhi Liu,[9] P. B. Mackenzie,[6] Y. Meurice,[12] E. T. Neil,[13,14] J. N. Simone,[6] R. Sugar,[15] D. Toussaint,[16] R. S. Van de Water,[6] and Ran Zhou[6]

(Fermilab Lattice and MILC Collaborations)

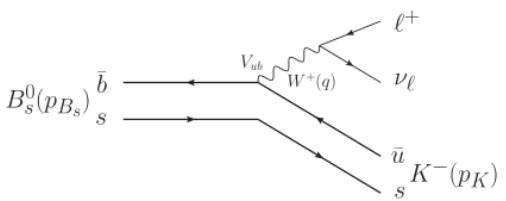

FIG. 1. Lowest order Standard Model Feynman diagram shown here for example of semileptonic $B_s^0 \to K^-\ell^+\nu_\ell$ decay.

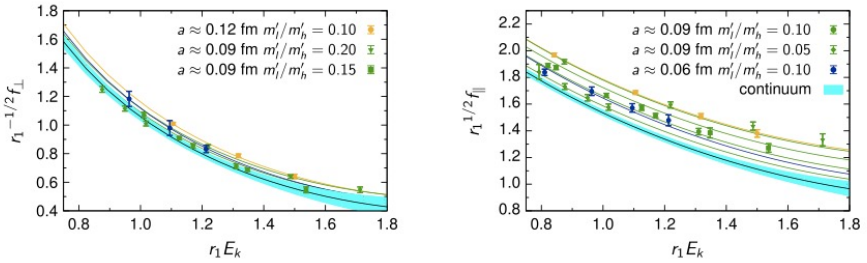

FIG. 7. Chiral-continuum extrapolated form factors $f_\parallel$ and $f_\perp$ in r_1 units as functions of the recoil energy $r_1 E_K$. The color denotes the lattice spacings and the symbols denote the ratio of the sea-quark masses m_l'/m_h'. The colored fit lines correspond to the fit results evaluated at the parameters of the ensembles. The cyan band with the black curve shows the chiral-continuum extrapolated results.

This lattice calculation predicted the shape of the differential decay rate for the B_s decay into a Kaon and leptons. After the analysis of the experimental data from LHCb is completed, it will provide a new determination of the CKM matrix element V_{ub}. Checking the unitarity of the CKM matrix is an important test of the standard model.
The CKM matrix relates mass and weak eigenstates.

bitstrings from QuEra: fast and unexpensive

[2]:
```
from braket.aws import AwsDevice
from pprint import pprint as pp

device = AwsDevice("arn:aws:braket:us-east-1::device/qpu/quera/Aquila")
```

Note: Some atoms may be missing even if the shot was successful. We recommend comparing `pre_sequence` of each shot with the req

[22]:
```
print("Quantum Task Summary")
print(tracker.quantum_tasks_statistics())
print('Note: Charges shown are estimates based on your Amazon Braket simulator and quantum processing unit (QPU) tas
print(f"Estimated cost to run this example: {tracker.qpu_tasks_cost() + tracker.simulator_tasks_cost():.2f} USD")
```

```
Quantum Task Summary
{'arn:aws:braket:us-east-1::device/qpu/quera/Aquila': {'shots': 100, 'tasks': {'COMPLETED': 1}}}
Note: Charges shown are estimates based on your Amazon Braket simulator and quantum processing unit (QPU) task usage
ts, and you may experience additional charges based on your use of other services such as Amazon Elastic Compute Clo
Estimated cost to run this example: 1.30 USD
```

[23]:
```
def get_counters_from_result(result):
    post_sequences = [list(measurement.post_sequence) for measurement in result.measurements]
    post_sequences = ["".join(['r' if site==0 else 'g' for site in post_sequence]) for post_sequence in post_sequenc

    counters = {}
    for post_sequence in post_sequences:
        if post_sequence in counters:
            counters[post_sequence] += 1
        else:
            counters[post_sequence] = 1
    return counters
get_counters_from_result(result)
```

[23]:
```
{'grrggrggrr': 1,
 'rggrgggggr': 7,
 'grrggggrrg': 7,
 'rrggggrggr': 6,
 'rrgggggrrg': 4,
 'grrgggggrr': 8,
 'rrgggrgrrg': 1,
 'rggrrggggr': 2,
 'rrggrggrrg': 2,
 'rrggggrrgr': 1,
 'rggrgrrggr': 1,
 'rggrrgrggr': 2,
 'rgrrggrggr': 1,
```

```
register = AtomArrangement()
ax = 4e-6  # meters
ay = 8e-6
ns=5
nl=2
for xx in range(ns):
    for yy in range(nl):
        register.add([xx*ax,yy*ay])

show_register(register)

#show_register(register, show_atom_index=False, blockade_radius= 1.5 * separation)
```

[6]:
```
#H += drive

from ahs_utils import show_global_drive
show_global_drive(drive)
```

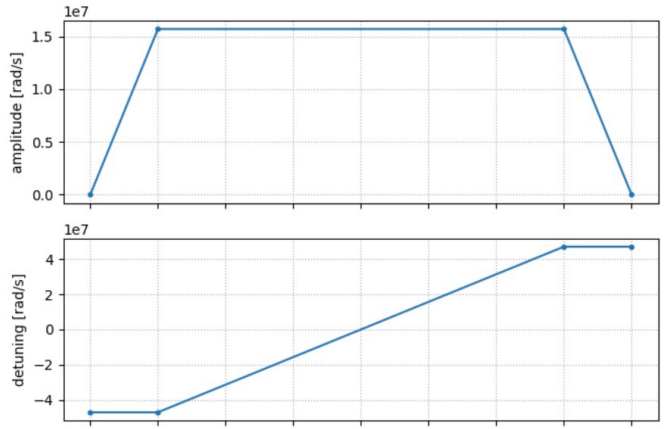

$S_A^{vN} \sim I_{AB}^X$ with Exact Diag. and Aquila (QuEra)
YM 2404.09935; PRR Letter 7, L022023 (2025)

Bitstring probabilities: $\langle\{n\}|\rho_{AB}|\{n\}\rangle = p_{\{n\}}$, bipartite: $\{n\} = \{n\}_A\{n\}_B$

Reduced bitstrings: $\langle\{n\}_A|\rho_A|\{n\}_A\rangle = p_{\{n\}_A} = \sum_{\{n\}_B} p_{\{n\}_A\{n\}_B}$

Bitstring Shannon entropy: $S_{AB}^X \equiv -\sum_{\{n\}} p_{\{n\}} \ln(p_{\{n\}})$

Reduced Shannon entropy: $S_A^X \equiv -\sum_{\{n\}_A} p_{\{n\}_A} \ln(p_{\{n\}_A})$

Classical mutual information (Shannon): $0 \leq I_{AB}^X \equiv S_A^X + S_B^X - S_{AB}^X$

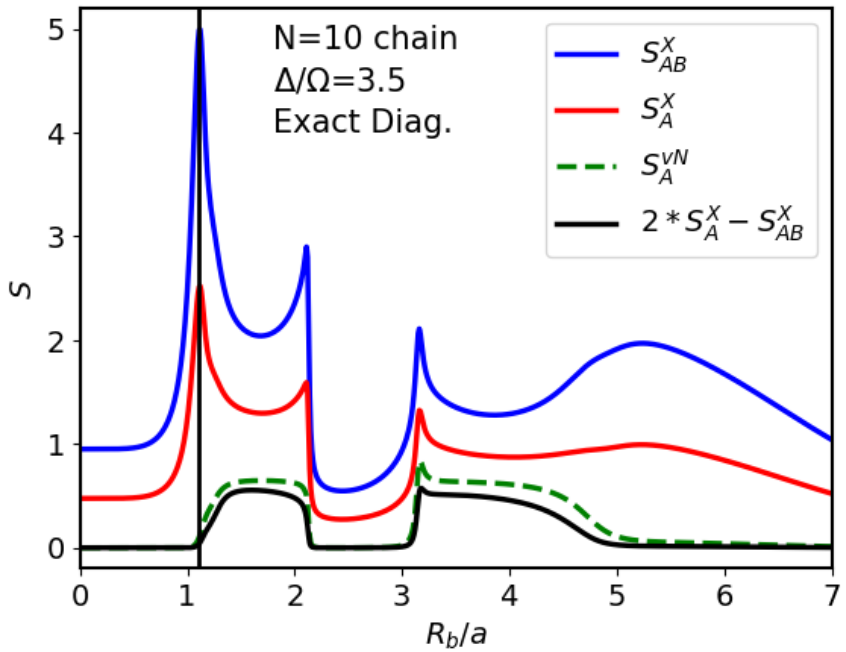

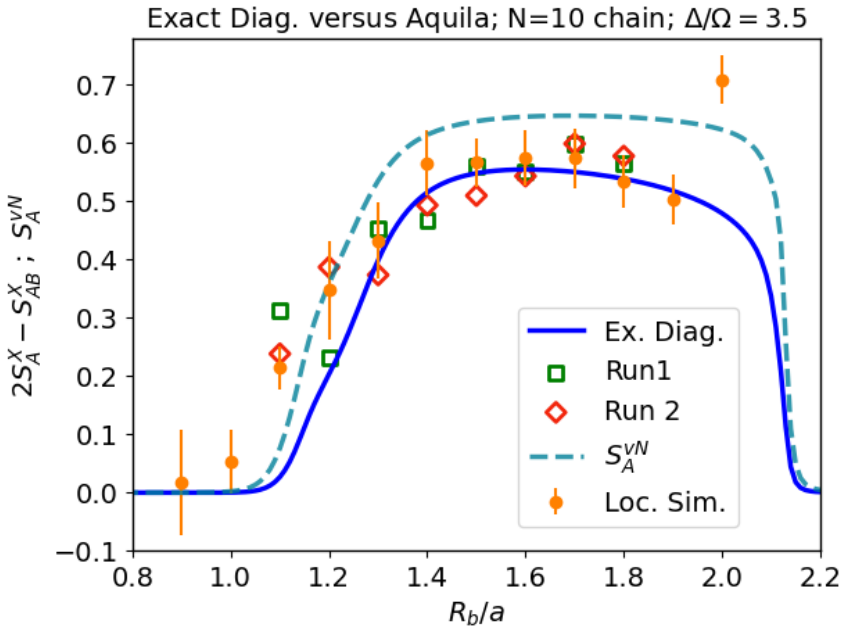

Bipartite rigorous inequalities (see YM 2404.09935)

- Density matrix of the vacuum of an AB system: $\rho_{AB} = |vac.\rangle\langle vac.|$
- Reduced density matrix: $\rho_A = \mathrm{Tr}_B \rho_{AB}$
- von Neumann entanglement entropy: $S_A^{vN} \equiv -\mathrm{Tr}(\rho_A \ln(\rho_A))$
- We want to estimate the entanglement with a single copy
- Bitstring probabilities: $\langle\{n\}|\rho_{AB}|\{n\}\rangle = p_{\{n\}}$, $\{n\} = \{n\}_A\{n\}_B$
- Reduced bitstrings: $\langle\{n\}_A|\rho_A|\{n\}_A\rangle = p_{\{n\}_A} = \sum_{\{n\}_B} p_{\{n\}_A\{n\}_B}$
- Bitstring Shannon entropy: $S_{AB}^X \equiv -\sum_{\{n\}} p_{\{n\}} \ln(p_{\{n\}})$
- Reduced Shannon entropy: $S_A^X \equiv -\sum_{\{n\}_A} p_{\{n\}_A} \ln(p_{\{n\}_A})$
- Classical mutual information (Shannon): $0 \leq I_{AB}^X \equiv S_A^X + S_B^X - S_{AB}^X$
- Diagonal upper bounds $S_B^{vN} = S_A^{vN} \leq S_A^X (\mathrm{or} S_B^X)$ (not sharp!)
- Holevo showed that $I_{AB}^X \leq S_B^{vN} = S_A^{vN}$

Summary: $0 \leq I_{AB}^X \leq S_B^{vN} = S_A^{vN} \leq S_A^X (\mathrm{or} S_B^X)$

Tightness of the MI (Holevo) bound

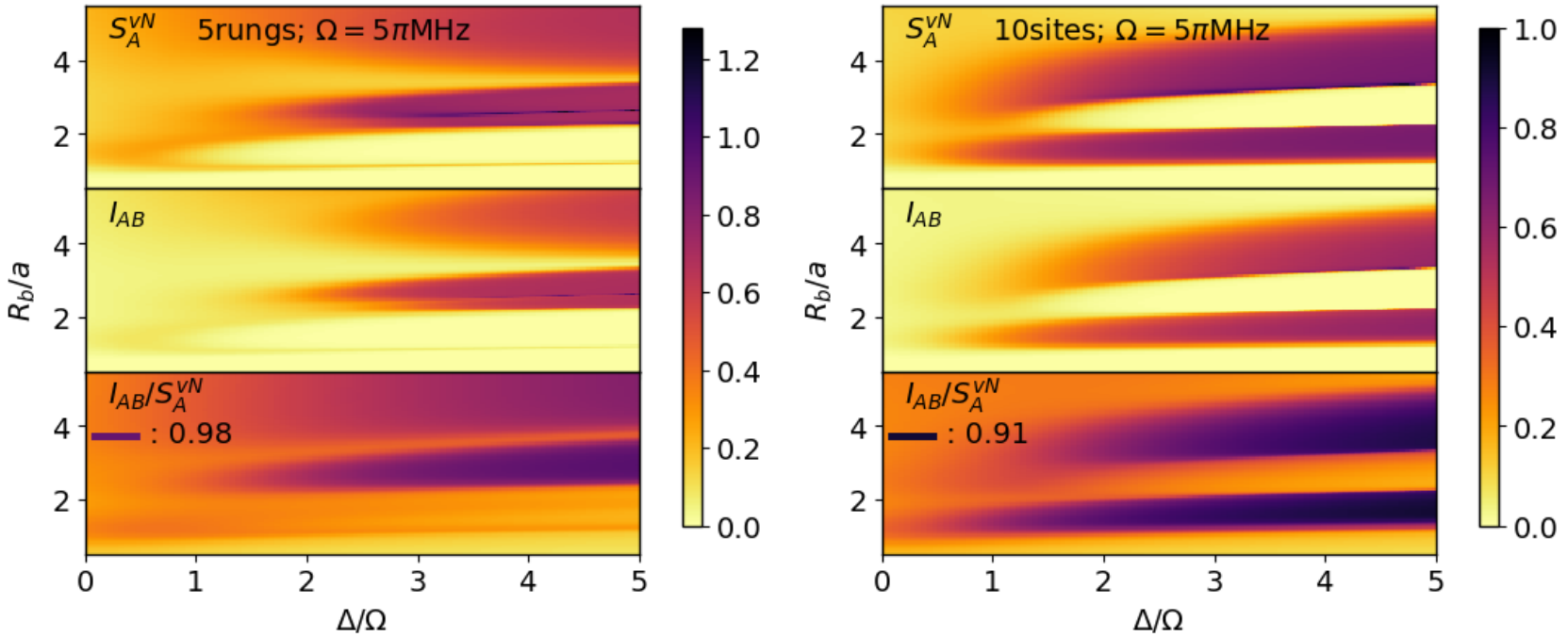

Figure: S^{vN}, I^X_{AB} and their ratio for a 10 sites chain (left) and a 5 rung ladder with $a_y/a_x = 2$ (right). The shapes of S^{vN} are similar to the shapes of I^X_{AB} but a bit darker. The bound is reasonably tight ($\sim$ 0.8-0.9 saturated when S^{vN} is large and not so tight when S^{vN} is small). I^X_{AB} is a good indicator for regions of large entanglement. We have used exact diagonalization for these figures, but I^X_{AB} can be easily obtained from empirical bitstrings. For details see arXiv 2404.09935; PRR 7, L022023.

Filtered probabilities

- Before measuring the occupation, you need to turn off Ω
- This need to be done fast or you end up adiabatically to the $\Omega = 0$ vacuum
- By turning Ω too slowly I noticed that it enhanced the high probabilities
- In this process, the mutual information got closer to S_A^{vN}!
- Then, we did it controllably by removing low probabilities and renormalizing (“filtering")
- Optimization: inflection point of conditional entropy
- Decent estimates of the quantum entanglement
- For details see Avi Kaufman, James Corona, Zane Ozzello, Blake Senseman, Muhammad Asaduzzaman, Yannick Meurice, Improved entanglement entropy estimates from filtered bitstring probabilities, arXiv:2411.07092, Phys. Rev. A 112, 032430

Effect of low probability truncation ("filtration")

see arXiv 2411.07092 Phys. Rev. A 112, 032430
Truncation/filtration: remove the bitstrings with
$p_{\{n\}} \simeq N_{\{n\}}/N_{shots} \leq p_{min}$ and renormalize.

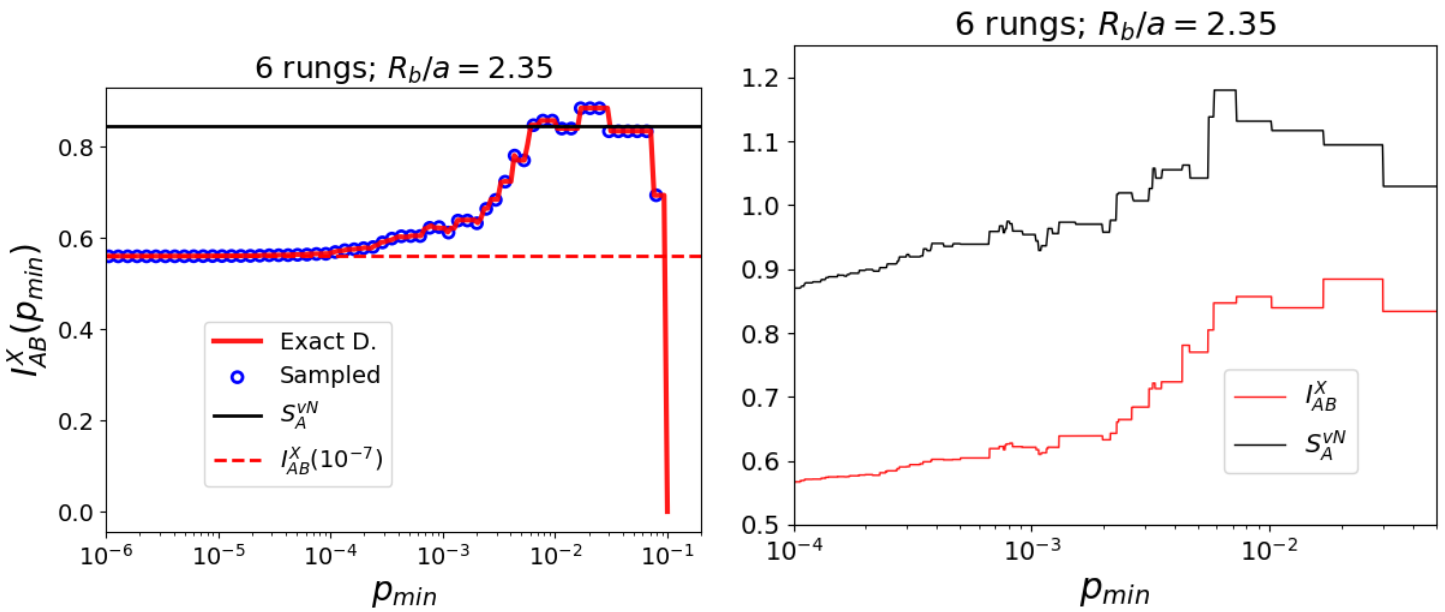

Figure: Left: $I^X_{AB}(p_{min})$ for a six-rung ladder with exact diagonalization (continuous red line) and DMRG sampling (blue open circles). Right: $I^X_{AB}(p_{min})$ and $S^{vN}_A(p_{min})$ for a six-rung ladder with exact diagonalization. If we project out the states corresponding to the truncated bitstrings, we have a new Hamiltonian and ground state: $I^X_{AB}(p_{min}) \leq S^{vN}_A(p_{min})$ (no contradiction).

Inflection point of conditional entropy

To filter the distribution effectively requires a scheme for determining when to stop. We have found the conditional entropy, another measure of correlation between subsystems, to provide a useful metric for sufficient filtering. The conditional entropy is defined as

$$S^X_{A|B} \equiv S^X_{AB} - S^X_B$$

and under filtering, it reduces gradually from an asymptotic initial value to zero. This curve is often well fit with a sigmoid (shifted hyperbolic tangent), the inflection point of which often lands very close to the optimal truncation value. This also closely corresponds to the location where $S^X_{A|B}$ has been reduced by half.

Optimized filtering (blows my mind!)

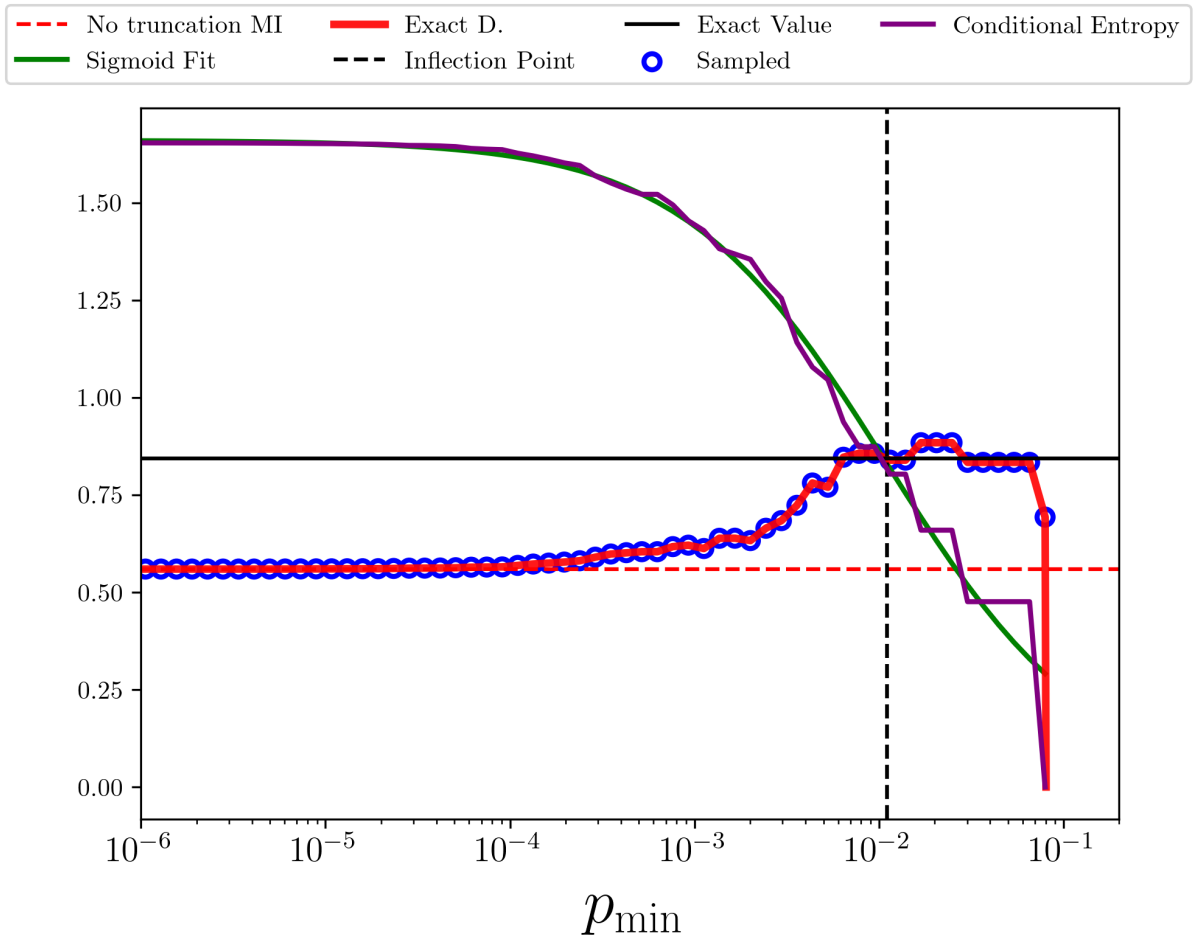

Figure: $I^X_{AB}(p_{min})$ for a six-rung ladder with exact diagonalization (continuous line) and DMRG sampling (open circles). Graph by Blake Senseman.

Optimized filtering

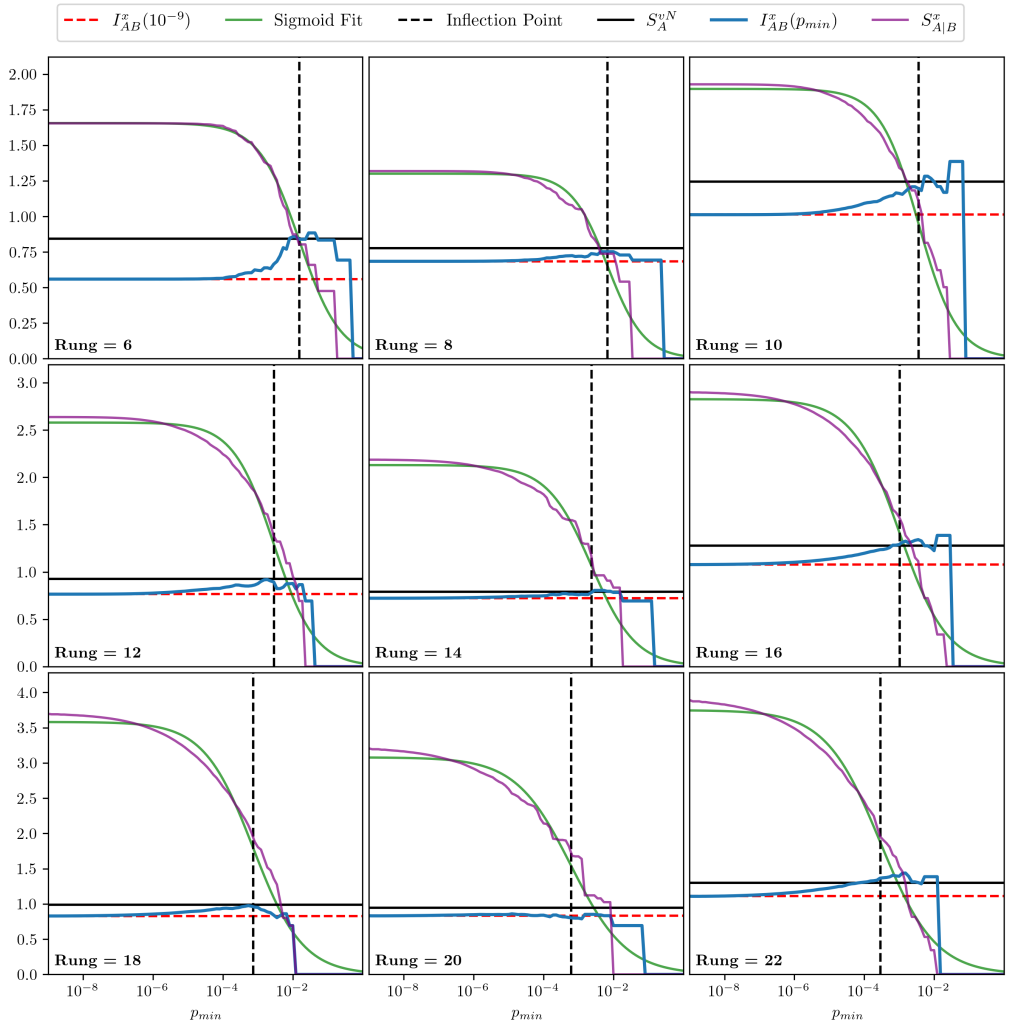

Figure: Effects of the system size on $I^X_{AB}(p_{min})$ for $R_b/a = 2.35$, 6,8...22 rungs obtained via exact diagonalization; comparing sigmoid and mid height.

QuEra bitstring probabilities

- Everybody can use QuEra (+ NERSC help)
- 1000 shots=\$10.3
- Easy to build dictionaries: $\{11010101011100 : 27, 00101000101010 : 7, ...\}$
- $p_{\{n\}} \simeq N_{\{n\}}/N_{shots}$, so the resolution is limited to $1/N_{shots}$.
- In a broad region of phase diagrams where the ground state is not obviously ordered or disordered, for a given N_{shots} and a sufficiently large system size, you end up seeing any given state at most once.
- States with very low (true) probabilities may be observed because of large multiplicities or experimental errors.
- We should try to have N_{shots} large enough to at least observe a few states more than once. This is a exponential cost with the size of the system!
- Interesting things to do: cumulative probabilities, density of probabilities and asymptotic behavior as $p \to 0$, filtration of observables (contributions from different probability sectors), multipartite entanglement and mutual information approximations.

Volume effects

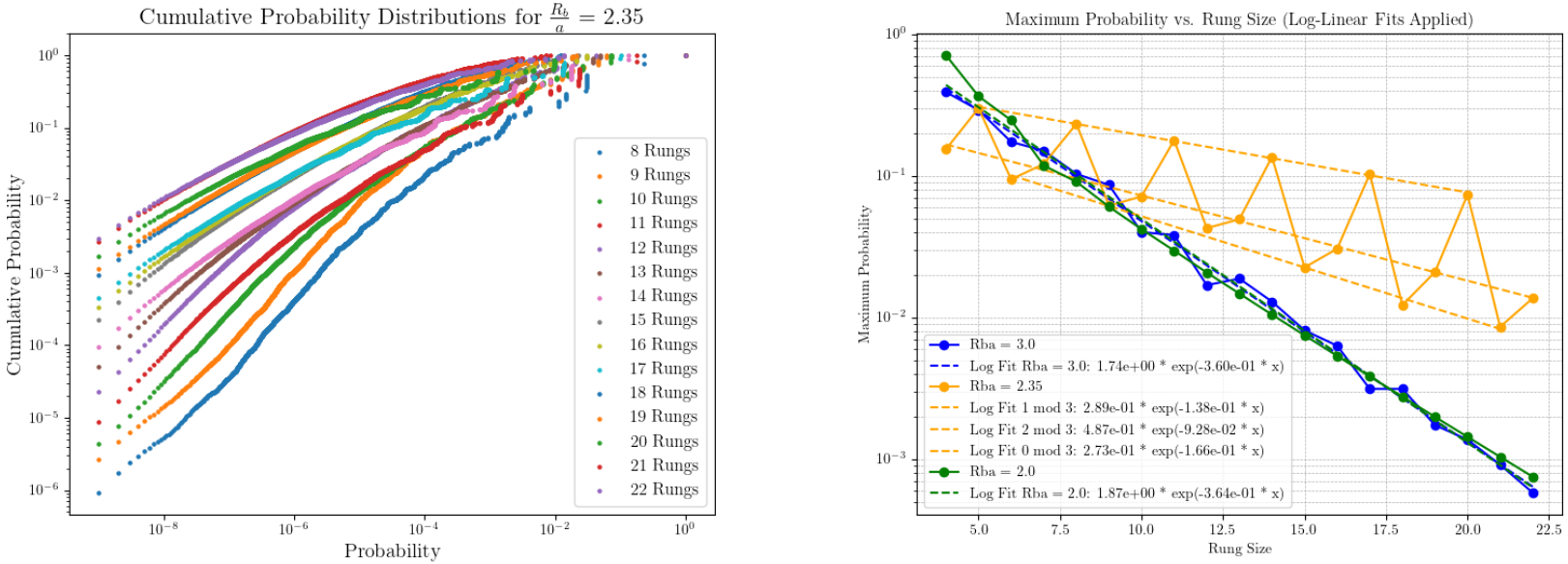

Figure: Cumulative probabilities tend to “move left" when the volume increases (approximate collapse). The largest probability appears to decrease exponentially with the size. Preliminary graphs by Avi Kaufman.

Executive summary of error analysis

1. Sorting fidelity: incorrect presequences can be removed by postselection. This leads to data loss that does not exceed 40% for the cases considered here. Getting close to $(0.995)^{N_{atoms}}$.
2. Adiabatic preparation: this is probably the main cause of errors. Longer rampup times seem to improve the situation for numerical calculations but not on the actual machine where longer preparation times have become available a few weeks ago. So there are things we don't know about experimental errors.
3. Ω Rampdown: a 0.05 μs is possible and only causes small errors compared to slower process.
4. Readout errors: they are very significant but they can be mitigated very efficiently after getting the bitstrings (M_3 method).

Progress in sorting fidelity

Fraction of correct presequences (no missing atoms)

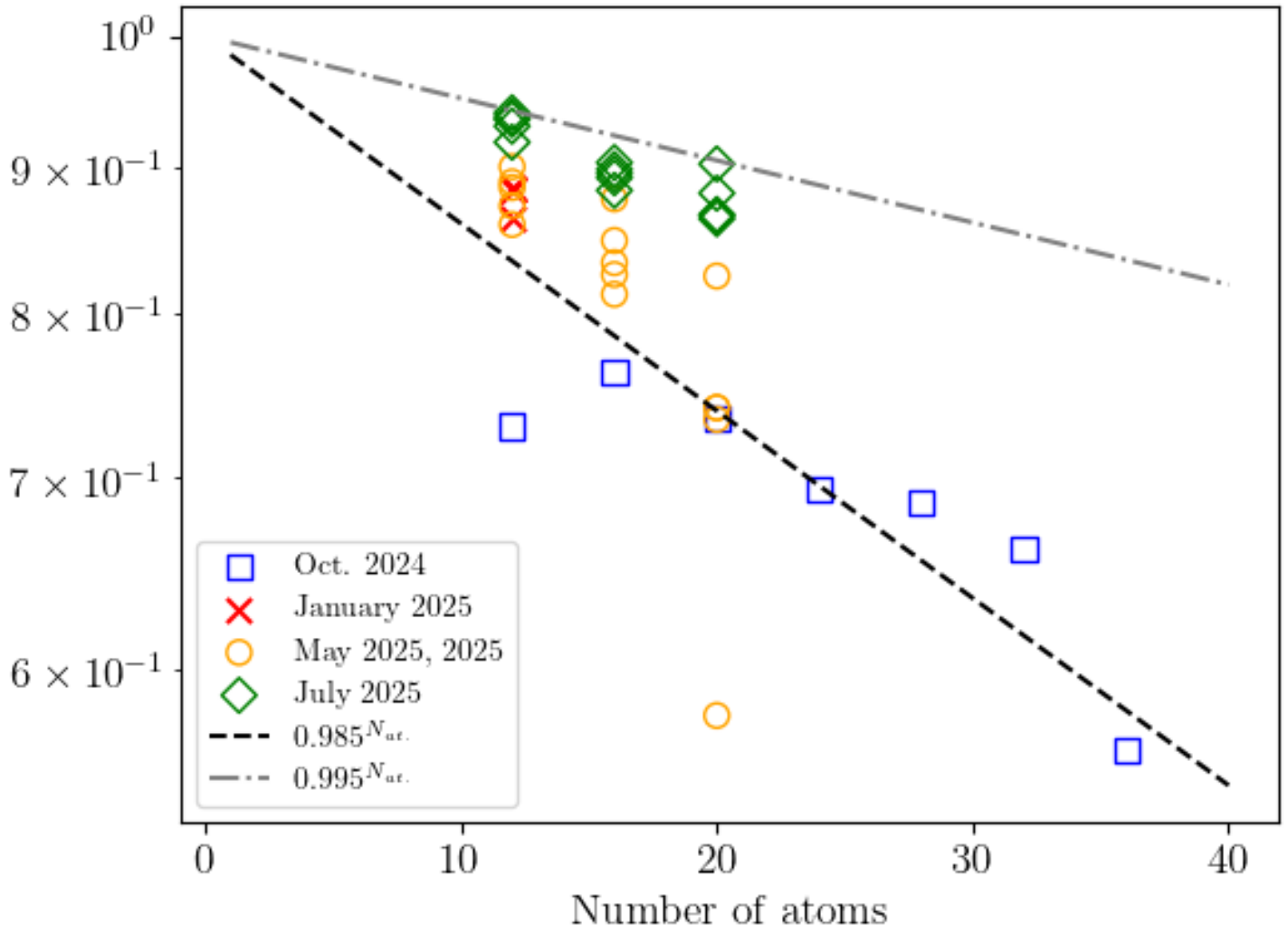

For details see Kaufman et al. arXiv: 2507.14128

Avi Kaufman is applying for grad. school (avi-kaufman@uiowa.edu)

Exploring near critical lattice gauge simulators with Rydberg atoms facilities

Avi Kaufman[1], James Corona[1], Zane Ozzello[1], Blake Senseman[1], Muhammad Asaduzzaman[1,2], and Yannick Meurice[1]
Department of Physics and Astronomy, The University of Iowa, Iowa City, IA 52242, USA and North Carolina State University, Department of Physics, Raleigh, NC 27607, USA
(Dated: July 21, 2025)

We motivate the use of a ladder of Rydberg atoms as an analog simulator for a lattice gauge theory version of scalar electrodynamics also called the compact Abelian Higgs model. We demonstrate that by using a few thousand shots from a single copy of the ladder simulator it is possible to estimate the bipartite quantum von Neumann entanglement entropy S_A^{vN}. The estimation relies on an optimized filtration of the mutual information associated with the bitstrings obtained from public facilities of configurable Rydberg arrays named Aquila. We discuss the limitations associated with finite sampling, sorting fidelity, adiabatic preparation, ramp-down of the Rabi frequency before measurement, and readout errors. We use cumulative probability distribution to compare Aquila results with high accuracy density matrix renormalization group (DMRG) or exact results. The state preparation appears to be the main source of error. We discuss the large volume behavior of the cumulative probability distribution and show examples where for a finite number of shots, there appears to be some large enough size for which any given state is seen at most once with high probability. We show that the results presented can be extended to multipartite entanglement. We briefly discuss the cost of the calculations for large square arrays in the context of obtaining quantum advantage in the near future.

I. INTRODUCTION

There has been a lot of recent interest for quantum simulation for models used in condensed matter, particle, and nuclear physics [1–7]. An area of focus is the real-time evolution for lattice gauge theory models [8–

Recent cold atom experiments [50, 51] have measured the second-order Rényi entropy by preparing twin copies of the ground state and applying the beamsplitter operation. One can measure the number of particles modulo 2 at each site j of a given copy (n_j^{copy}) [50], and use the result from [52]

Rubidium vs. Strontium (or soon Ytterbium)

with Avi Kaufman and Joonhee Choi (preliminary with 6 atoms)

Cumulative probabilities: $\Sigma(p_\Lambda) = \sum_{\{n\}:p_{\{n\}}\leq p_\Lambda} p_{\{n\}}$.
Probability to observe any state having a probability less than p_Λ.
Strontium data from arXiv:2308.07914, Nature 628, 71-77 (2024), Benchmarking highly entangled states on a 60-atom, ... by Adam L. Shaw, Zhuo Chen, Joonhee Choi, Daniel K. Mark, Pascal Scholl, Ran Finkelstein, Andreas Elben, Soonwon Choi, and Manuel Endres.

Quick search for critical points with multipartition?

- $S_{weak} = S_{AB} + S_{BC} - S_A - S_C \geq 0$ (weak monotonicity)
- $S_{strong} = S_{AB} + S_{BC} - S_B - S_{ABC} \geq 0$ (strong subadditivity)
- Cancellation of IR and UV contributions in 1+1 dimensions
- Appear to spot phase boundary more sharply
- Mutual information approximation, filtration and optimization from conditional entropy work.
- see Zane Ozzello and YM, arxiv 2507.14422

CFT and multipartition: Lin and McGreevy (PRL 131)

A linear combination of entanglement

$$S_\Delta := (S_{AB} + S_{BC}) - \eta(S_A + S_C) - (1-\eta)(S_B + S_{ABC})$$

where $\eta = \frac{(x_2-x_1)(x_4-x_3)}{(x_3-x_1)(x_4-x_2)}$ with partition edges x_i, has remarkable extremal properties and is a convex combination of the nonnegative quantities S_{weak} and S_{strong}.

$$\begin{aligned} S_{weak} &= S_{AB} + S_{BC} - S_A - S_C \geq 0 \\ &\simeq I_{AB} + I_{BC} - I_A - I_C \\ &= H_{AB} + H_{CD} + H_{BC} + H_{AD} - H_A - H_{BCD} - H_C - H_{ABD} \end{aligned}$$

$$\begin{aligned} S_{strong} &= S_{AB} + S_{BC} - S_B - S_{ABC} \geq 0 \\ &\simeq I_{AB} + I_{BC} - I_B - I_{ABC} \\ &= H_{AB} + H_{CD} + H_{BC} + H_{AD} - H_B - H_{ACD} - H_{ABC} - H_D. \end{aligned}$$

See also their arXiv:2509.04596, A systematic search for conformal field theories in very small spaces.

Sharper localization of critical points

Zane Ozzello and YM, arxiv 2507.14422

$$\hat{H}_{\text{Ising}} = -h\sum_{i=1}^{N_s}\hat{\sigma}_i^z - J\sum_{i=1}^{N_s}\hat{\sigma}_i^x\hat{\sigma}_{i+1}^x.$$

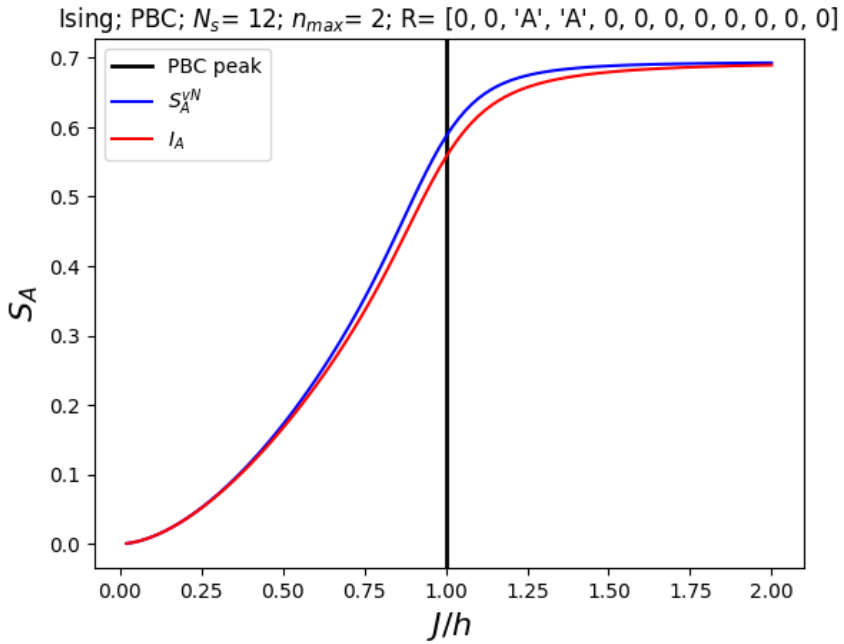

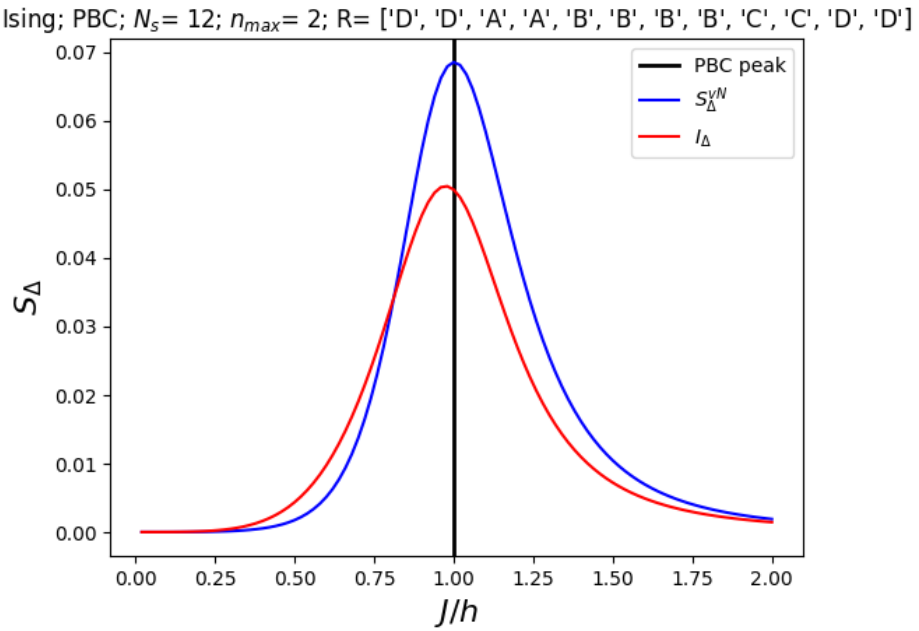

See also ϕ^4 and Rydberg chains.

Filtering works!

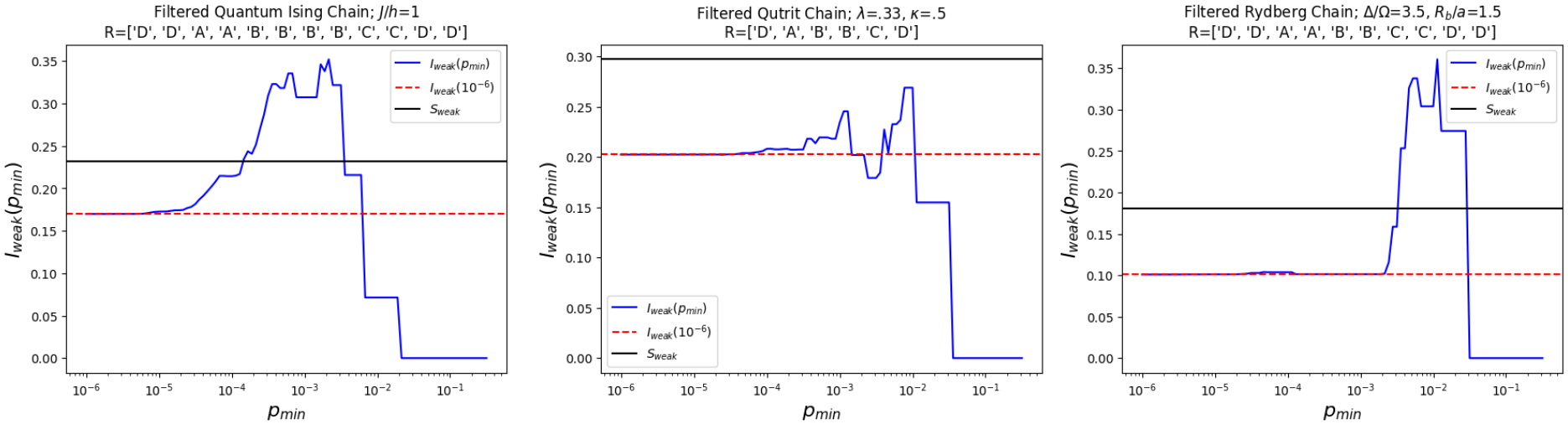

Figure: From left to right, filtering applied to Ising, ϕ^4, and Rydberg chain systems

Optimization with conditional probability also seems to work. Z. Ozzello, preliminary work.

For details see Z. Ozzello and YM arXiv: 2507.14422

Zane Ozzello will be applying for postdoc in Fall 2026 (zane-ozzello@uiowa.edu)

Multipartite entanglement from ditstrings for 1+1D systems

Zane Ozzello and Yannick Meurice

Department of Physics and Astronomy,

The University of Iowa, Iowa City, IA 52242, USA

(Dated: July 22, 2025)

Abstract

We show that multipartite entanglement can be used as an efficient way of identifying the critical points of 1+1D systems. We demonstrate this with the quantum Ising model, lattice $\lambda\phi^4$ approximated with qutrits, and arrays of Rydberg atoms. To do so we make use of multipartite compositions of entanglement quantities for different parts combined to form the strong subadditivity, weak monotonicity, and a convex combination of these with conformal properties. These quantities display some remarkable properties. We will demonstrate how the entanglement of individual parts together displays behavior at phase boundaries, but the combination of these in the aforementioned quantities sharpens and localizes this behavior to the boundaries even better. We will show that we can extend a scheme for approximating the entanglement with the mutual information, and that this acts as a lower bound which will also follow the changes in the entanglement for the above quantities, despite the additional contributions of different signs. This mutual information approximation to the identifying quantities can have its lower probabilities removed in a process we call filtering, and despite the combination of terms will respond well to the filtering and offer improvements to the lower bound.

Particle Multiplicity (graph by K. Heitritter, 2212.02476)

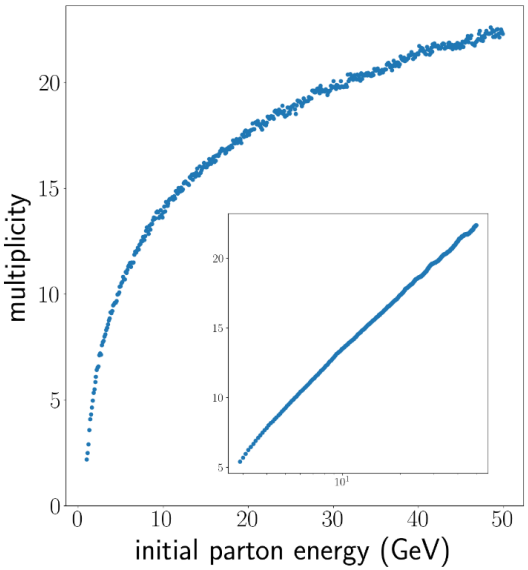

Pythia/Lund

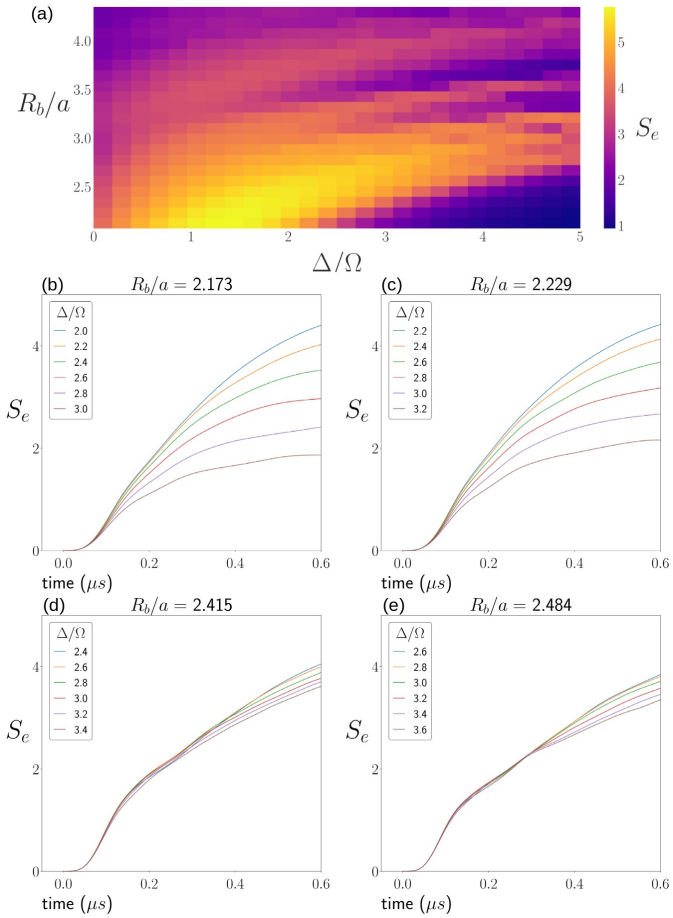

Entanglement Entropy (simulator)

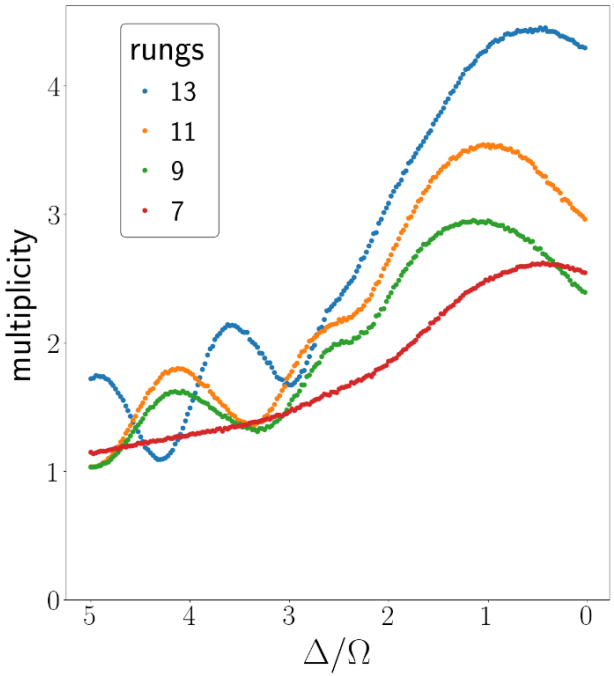

First attempt on a small lattice with detuning playing the role of energy
(see arxiv 2212.02476)

Preparing high multiplicity states using $\Delta > 0$

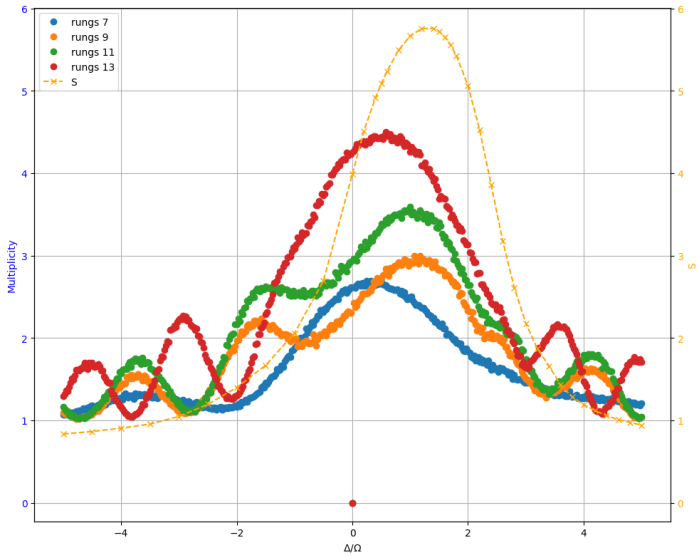

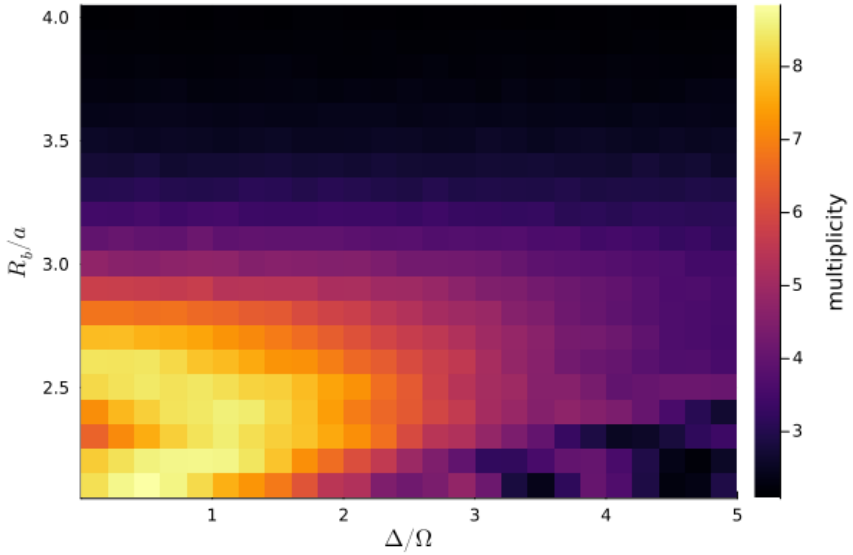

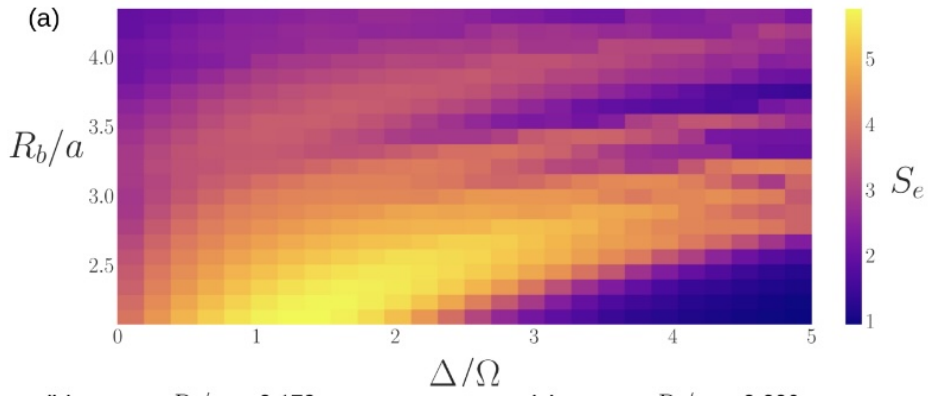

Particle multiplicity (top) and entanglement entropy (bottom) (graphs by Heitritter, Senseman, Ozzello, see 2212.02476 for particle production; time scales under reconsideration.)

Conclusions

- Matching between simulator (ladder of Rydberg atoms) and target model (scalar QED) should be understood in the continuum limit.
- Effective Hamiltonians for the simulator: same three types of terms as the target model plus an extra quartic term.
- The two-leg ladder has a very rich phase diagram.
- First experimental observation of the floating phase.
- Mutual information from bitstrings: good estimation of the order of magnitude of the von Neumann quantum entanglement S_A^{vN}.
- Bitstrings: e. g., 0101101011 is measured 78 times in 1000 shots, are easy to obtain from a single copy.
- Filtration of probabilities improves the bound; optimization using conditional entropy (systematic understanding in progress).
- Device errors under control, bi-partite estimates
- Multipartite estimates
- Thanks for listening!
- For questions, email: yannick-meurice@uiowa.edu .

Cumulative probabilities

A simple way to characterize the importance of the low-probability states is calculate their probability weighted sum below some maximal value p_Λ

$$\Sigma(p_\Lambda) = \sum_{\{n\}:p_{\{n\}}\leq p_\Lambda} p_{\{n\}}.$$

This quantity is the probability to observe any state having a probability less than p_Λ. If we sample the distribution N_{sh} times, we expect to observe $N_{sh}\Sigma(p_\Lambda)$ states having a probability less than p_Λ.
This cumulative probability distribution can be estimated by using N_{sh} measurements and counting the number of times $N_{\{n\}}$ a state $|\{n\}\rangle$ is observed. We then have an approximation for the occupation probability

$$p_{\{n\}} \simeq N_{\{n\}}/N_{sh}.$$

M_3 restores the initial distribution with good accuracy

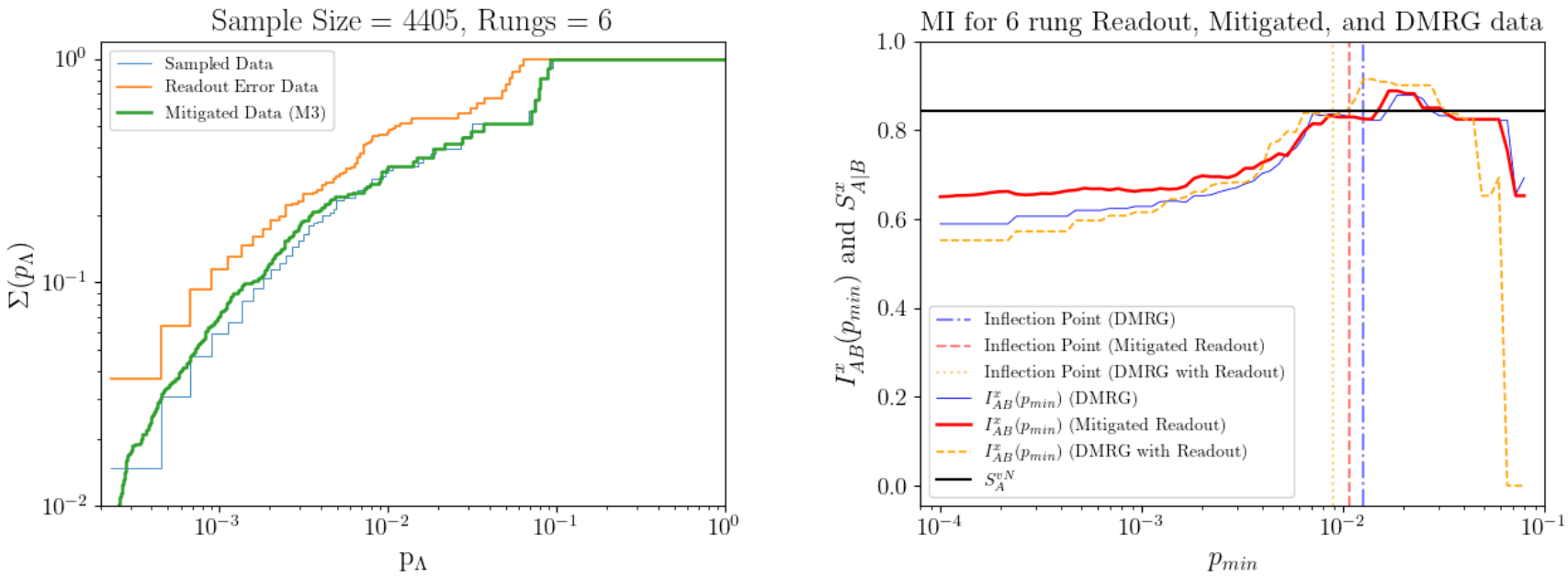

Figure: Comparison of cumulative distributions (left) and mutual information (right) for the 6-rung ladder. (No Hardware Data).